Determination of Both Tilting and In-Plane Molecular Rotational Angles for Dinaphtho[2,3-*b*:2',3'-*f*]thieno[3,2-*b*]thiophene Using Near Edge X-ray Absorption Fine Structure

AUTHOR NAMES

Kazuaki Iwasawa[1], Yuu Urabe[1], Keisuke Honya[1], Hiroyuki Yoshida[2,3], and Koji K. Okudaira[,2]*

Affiliation

1. Graduate School of Advanced Integration Science, Chiba University, 1-33 Yayoi-cho, Inage-ku, Chiba 263-8522, Japan

2. Graduate School of Engineering, Chiba University, 1-33 Yayoi-cho, Inage-ku, Chiba 263-8522, Japan

3. Molecular Chirality Research Center, Chiba University, 1-33 Yayoi-cho, Inage-ku, Chiba 263-8522, Japan

Abstract

We demonstrate that both the in-plane molecular rotational and the tilting angles of the molecular orientation can be determined using the σ* resonance of sulfur (S) K-edge near edge X-ray absorption fine structure. We examined dinaphtho[2,3-*b*:2',3'-*f*]thieno[3,2-*b*]thiophene (DNTT) thin films on silicon dioxide (SiO_2) and copper oxide (CuO_x) substrates which are relevant to the cost-effective organic field-effect transistors. In-plane directed transition moments were attributed to the electron excitation from S 1s to largely overlapped σ* orbital related to the C-S bonding at the thiophene site. Under the coexistence with a minor component of the amorphous region, it turned out that the DNTT domain with the single crystal structure with the c-axis normal to the substrates; the DNTT molecules on SiO_2 orient at a tilting angle (β) of 85° and an in-plane rotational angle (Φ_M) of 77° and 103°. In the case of the film on CuO_x, values of 84° for β, 73° and 107° for Φ_M are acquired. The amount of amorphous region in the film on CuO_x was larger than that on SiO_2. Our approach is applicable to other sulfur-containing molecules with a small population of the lowest unoccupied molecular orbital on the S atoms.

Introduction

The use of organic semiconductors has been extensively explored for the conductive channel layer in organic field-effect transistors (OFETs). Since the carrier mobility of organic solid is highly anisotropic, the molecular orientation in the conductive channel greatly affects the

performance of OFET. The molecular orientation also affects the energy levels of organic semiconductor films due to the electrostatic interaction.[1–3]

The molecular orientation has been routinely investigated by means of diffraction techniques such as X-ray diffraction (XRD) and low energy electron diffraction (LEED) for long-range ordered thin films.[4,5] Although the XRD is useful for crystalline films, it is generally not a suitable method to analyze detailed molecular orientation in amorphous films due to the lack of diffraction spots. LEED gives the lattice constants along the substrate plane. However, the radiation damage of molecules may be occurred by the electron beam. Scanning tunneling microscopy (STM) examining the outmost molecular orbitals provides information on the molecular orientation at extremely low temperatures.[5,6] This is not the case for the interest on the molecular orientation at room temperature. In contrast, near edge X-ray absorption fine structure (NEXAFS) has a great advantage to analyze the molecular orientation of both the crystalline and amorphous regions in thin organic layers. NEXAFS acquires signals from an individual molecule due to the transition from the core-level to the unoccupied states with high sensitivity.[7] The molecular orientation can be determined by analyzing the polarization dependence of NEXAFS spectra.

The polarization dependence of carbon (C) K-edge NEXAFS with the C1s to π* transition is usually applied to analyze the molecular orientation. The experimental geometry is shown in Figure 1a. In this measurement, the transition from the C1s core level to π* unoccupied level is examined as a function of the incident angle (α). As the transition dipole is normal to the molecular plane, only the tilting angle (β) of the molecular plane with respect to the substrate can be determined.[8] However, the information about the molecular rotational angle (Φ_M) is missing,

which is insufficient to discuss the favorable molecular orientations in the conductive channel of OFET. In order to fully determine the molecular orientation, additional data to complement Φ_M is required. For example, DNTT thin films were examined by the C K-edge NEXAFS in previous studies where the molecular orientation was confirmed with the aid of XRD.[9,10]

So far, Φ_M in the molecular plane has never been reported by NEXAFS. If Φ_M is determined, the molecular orientation can be derived using only NEXAFS, which gives us full advantages of the high sensitivity and detection of crystalline/amorphous regions of NEXAFS. This can be achieved by observing the σ* resonance whose transition dipole lies along the molecular plane. Usually, the σ* state of the organic molecule locates at higher energies and has the shorter lifetime than the π* state. Thus, the peak of the σ* resonance in NEXAFS is difficult to analyze because of the strong background signal and broadened peak shape. Further, the σ* resonances within the molecular plane may consist of transitions in various directions. It is normally difficult to determine the molecular orientation solely from the NEXAFS data.

In the study, we demonstrate that the molecular orientation of dinaphtho[2,3-*b*:2',3'-*f*]thieno[3,2-*b*]thiophene (DNTT; Figure 1b) films can be derived using the incident angle dependence of sulfur (S) K-edge NEXAFS spectra. DNTT has an enlarged π molecular orbital owing to the S atoms at the center of the molecule,[11–13] exhibiting the high carrier mobility in DNTT-based OFETs.[14–22] The larger ionization energy (5.4eV) provides an improved air-stability of OFET compared with that of typical OFT material, e.g. pentacene (5.0eV).[21] We observe sharp doublet peaks in the spectra which can be decomposed into the transition along with the molecular short (*x'*) and long (*y'*) axes based on a density functional theory (DFT) calculation including the anisotropic components of transition moment. From the

analysis, we successfully determine both the tilting β and rotational Φ_M angles using only the S K-edge NEXAFS. The present results are further confirmed by 2D-grazing incidence X-ray diffraction (XRD) measurements.

NEXAFS spectra of DNTT were acquired on silicon dioxide (SiO_2) and copper oxide (CuO_x) substrates. These substrates were chosen, aiming at the future application to a cost-effective and solution-processed OFET with the bottom-contact type structure fabricated in the air. Fine pitch patterning of source/drain contacts based on the established silicon semiconductor processes such as the copper damascene structure, depicted in Figure 1c, can facilitate large-scale integration of small OFETs.[23] In view of such a finely structured surface, the molecular orientation in organic semiconductor thin films on oxidized metal electrodes such as CuO_x should be investigated as well as that on an insulating SiO_2.

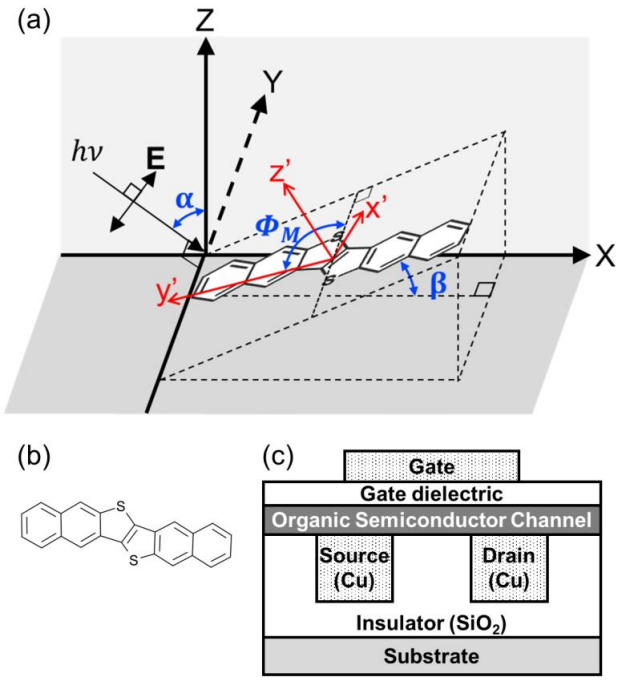

Figure 1. Schematic illustrations of (a) the experimental geometry for NEXAFS measurements, (b) the chemical structure of DNTT, and (c) a bottom-contact type OFET. The symbols of X, Y, and Z denote the laboratory coordinates. Besides, the symbols of x', y', and z' represent the molecular coordinates. The dotted line around the molecule shows a guide for the eye. Inorganic oxides such as SiO_2 and AlO_x, and organic insulating films are given as examples of the gate dielectric layer.

Experiment

The SiO_2 substrates were prepared by UV-O_3 oxidation of the silicon (100) surface. The polycrystalline copper films on silicon (100) deposited by immersion in plating solution were oxidized by the UV-O_3 process to form CuO_x substrates. DNTT (sublimed grade, 99% purity) without additional purification applied to sample preparation. 1.5-nm-thick DNTT thin films, corresponding to the monolayer thickness along the long molecular axis were deposited on the SiO_2 and CuO_x substrates by vacuum evaporation at room temperature. The film thickness was measured using a quartz thickness monitor. A 6nm-thick DNTT thin film on SiO_2 was prepared for the additional sample in the same manner. After deposition, the samples were exposed to the air and then introduced to the vacuum chamber for S K-edge NEXAFS measurement. No degradation of the thin film was observed by ultraviolet photoelectron spectroscopy (supporting information).

NEXAFS experiments were conducted at beamline 27A of the Photon Factory, the High Energy Accelerator Research Organization, Tsukuba. S K-edge NEXAFS spectra of 1.5-nm-thick DNTT thin films on silicon dioxide (SiO_2) and copper oxide (CuO_x) substrates

were acquired by means of the total electron yield (TEY) mode at a pressure of 8.0×10^{-7} Pa. All measurements were performed at room temperature.

In the analysis, the molecular orientation was determined from the polarization dependence of NEXAFS spectra, in which incident angle dependence of linearly polarized X-ray was analyzed. As depicted in Figure 1a, α is defined as the angle between the incident X-ray and the surface normal. β expresses the degree of the inclined molecular plane from the reference substrate surface. Φ_M shows the degree of in-plane rotation at the molecular plane. Here, $\Phi_M = 0°$ corresponds to a condition in which molecular long axis projection onto the surface is perpendicular to the electrical vector of the incident photon (**E**). $\Phi_M = 90°$ corresponds to the parallel condition. In molecular coordinates, decomposed x'-, y'-, and z'-direction components of the electronic transition intensity, which were denoted $I_{x'}$, $I_{y'}$, and $I_{z'}$, respectively, were quantitatively described as follows,[7]

$$I_{x'}(\alpha, \Phi_M, \beta) \propto \pi(\cos^2\alpha\, cos^2\Phi_M \cos^2\beta + \cos^2\alpha\, sin^2\Phi_M + 2\sin^2\alpha\, cos^2\Phi_M \sin^2\beta)$$
$$I_{y'}(\alpha, \Phi_M, \beta) \propto \pi(\cos^2\alpha\, sin^2\Phi_M \cos^2\beta + \cos^2\alpha\, cos^2\Phi_M + 2\sin^2\alpha\, sin^2\Phi_M \sin^2\beta)$$
$$I_{z'}(\alpha, \Phi_M, \beta) \propto \pi(\cos^2\alpha \sin^2\beta + 2\sin^2\alpha \cos^2\beta) \quad (1)$$

We assumed here that there was no azimuthal anisotropy regarding the arrangement of the outermost atoms on SiO_2 and CuO_x substrates. The composition ratio of the components contained in a transition peak from S 1s to the unoccupied state was obtained by NEXAFS simulation. A spectral simulation of NEXAFS was performed by DFT calculation with the

functional of Perdew and Wang (PW86/PW91) on the StoBe-DEMON program[24,25]. The S 1s core-hole state was described by a basis set of the triple zeta (73111/6111/1).

XRD measurement was carried out at beamline BL46XU of SPring-8. The wavelength of the incident X-ray was 0.1 nm.

Results and discussion

Figure 2 shows S K-edge NEXAFS spectra of DNTT on (a) SiO_2 and (b) CuO_x substrates at α = 0 (normal incidence), 10, 20, 30, 40, 50, and 60° (grazing incidence). In Figure 2a and 2b, three features at $h\nu$ = 2473, 2475, and 2479 eV were clearly detected on both the SiO_2 and CuO_x substrate at α = 0°. The feature at $h\nu$ = 2482eV detected only on CuO_x was assigned to $CuSO_4$ originated from the copper plating solution.[26] Energy positions of the features at $h\nu$ = 2473, 2475, and 2479 eV on SiO_2 are in good agreement with those on the CuO_x substrate. The broad features at 2479 eV whose intensity has little dependence on the incident angle were assigned to a transition from the S 1s to the σ* quasi-continuous states. The intensities of the first two peaks show the angular dependence on the incident photon. As the incident angle increases, the first peak at $h\nu$ = 2473 eV becomes stronger, while the second peak at $h\nu$ = 2475 eV becomes weaker.

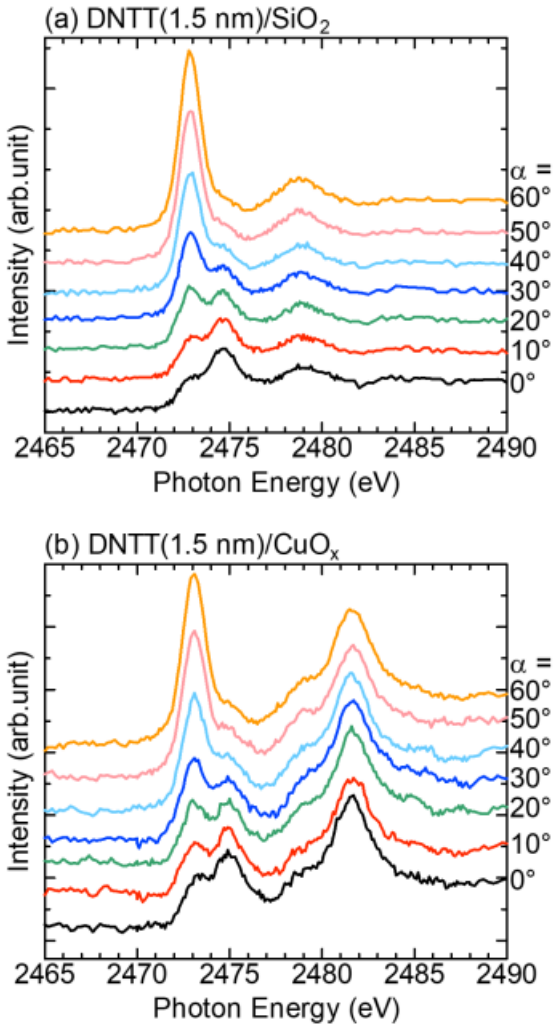

Figure 2. S K-edge NEXAFS of 1.5-nm-thick DNTT films on (a) SiO_2 and (b) CuO_x substrates. Spectra shown with vertical offset were acquired at a range of the incident angles (α) between 0° (normal incidence) and 60° (grazing incidence).

To analyze the angular dependence, a relationship between the molecular axes and the transition moment in the electron excitation process was firstly considered.[7,8] Generally, the transition moment from the C K-edge inner shell to the π* state in π-conjugated planar molecules

is normal to the molecular plane since the population of lowest unoccupied molecular orbital (LUMO) for the π* state is mainly distributed over the delocalized aromatic rings. However, LUMO of DNTT is mostly populated on the naphthalene rings while absent on the S atoms.[27] A small overlap of wave functions between the S 1s inner shell and LUMO should provide almost no electronic transition perpendicular to the molecular plane from the S 1s to LUMO. On the other hand, the transition moment parallel to the molecular plane can occur in the excitation from S 1s to largely overlapped σ* orbital located at the C-S bonding of the tienotiophene site. It implies that the peaks at 2473 eV and 2475 eV have the transition moment parallel to the molecular plane.

For further examination of the angular distribution of peaks at $h\nu$ = 2473 and 2475 eV, we calculated the electronic transition intensity of the isolated molecule by means of DFT calculation using StoBe-DEMON program.[24,25] Figure 3a shows a comparison between the observed and calculated NEXAFS spectra of DNTT. The calculated NEXAFS spectrum reproduces well the two peaks at 2473 eV and 2475 eV in the experiment. It indicated that the molecule-substrate interaction was weak. In a system where the molecule-substrate interaction is strong, the simulation may be different from that of the isolated molecule. Figure 3b shows the transition intensities along the molecular coordinates x', y', and z' (the coordinates are given in Figure 1) together with the simulated spectra. It is clear that these two peaks contain only the x' and y' components ($I_{x'}$ and $I_{y'}$). These in-plane transition moments can be attributed to the electron excitation from S 1s to largely overlapped σ* orbital related to the C-S bonding at the tienotiophene site. The transition moment of the first peak is almost along the molecular long axis with $I_{x'}$:$I_{y'}$ = 1:5. On the contrary, the second peak, which consists of two x' components and

one y' component, is close to the molecular short axis with $I_{x'}$:$I_{y'}$ = 3.5:1. Based on the ratio of $I_{x'}$:$I_{y'}$ in Figure 3 (b), the transition intensity $I_1(\alpha, \Phi_M, \beta)$ of the first peak is described as follows:

$$I_1(\alpha, \Phi_M, \beta) = \frac{1}{6} I_{x'} + \frac{5}{6} I_{y'} \quad (2)$$

The transition intensity $I_2(\alpha, \Phi_M, \beta)$ of the second peak is written in the same manner,

$$I_2(\alpha, \Phi_M, \beta) = \frac{7}{9} I_{x'} + \frac{2}{9} I_{y'} \quad (3)$$

Multiple combinations of tilting and rotation angles are separately obtained from the polarization dependence for either eqs 2 or 3. For a virtual combination of β = 86° and Φ_M = 73° in the analysis using eq 2 alone, the same polarization dependence is reproduced by other angles such as β = 74.3° and Φ_M = 90°, widening the range of the solution. Instead, the range can be narrowed by the simultaneous analysis using both eqs 2 and 3. the polarization dependence of eq 3 is distinguishable for the combinations above, since transition moments of the first and second peaks point in different directions each other in the molecular plane.

In addition, the polarization dependence is averaged in the coexistence of both the crystalline and amorphous regions, since all molecules in the specimen are reflected in the NEXAFS spectrum. To give an exact determination of the molecular orientation, it is effective to

incorporate the composition of the amorphous region into the analysis. The flat-lying molecules, as well as the randomly oriented molecules, can be assigned to the amorphous region since the flat-lying molecules have an isotropic distribution with respect to the in-plane rotation. For the flat-lying molecules, the first and second peaks show the same reduced polarization dependence. Under the condition of $\beta = 0$ in eqs 2 and 3, the transition intensity, $I_1 = I_2 \propto \pi \cos^2 \alpha$, is independent of Φ_M. It indicates that all molecules in the flat-lying orientation are inspected as equivalent. In the case of randomly oriented molecules, Φ_M is averaged to be 45° or 135°, so that the polarization dependence of the first peak is in perfect agreement with that of the second peak. As for the tilting angle, $\beta = 57.3°$ is derived from the three-dimensional isotropic random orientation model, revealing a slightly increasing polarization dependence.[28] For instance, a virtual configuration in the thin film, consisted of 90% standing ($\beta = 90°$ and $\Phi_M = 90°$) and 10% flat-lying ($\beta = 0°$) molecules, results in number-average values of $\beta = 72°$ and $\Phi_M = 90°$. In addition, the values of $\beta = 80°$ and $\Phi_M = 79°$ are derived when coexisting 90% standing molecules ($\beta = 90°$ and $\Phi_M = 90°$) and 10% randomly oriented ones ($\beta = 57.3°$ and $\Phi_M = 45°$).

Figure S2a (supporting information) shows $I_1(\alpha, \Phi_M, \beta)$ and $I_2(\alpha, \Phi_M, \beta)$ for various combinations of β and Φ_M (The definitions of α, β, and Φ_M are given in Figure 1a). The calculated $I_1(\alpha, \Phi_M, \beta)$ for any Φ_M decreases or shows no change as α increases in the range of $\beta = 0$–40°. In the range of $\Phi_M = 0$–30° (150–180°), $I_1(\alpha, \Phi_M, \beta)$ decreases or shows no change as α increases for any β. On the other hand, the experimental intensities of the first peak in S K-edge NEXAFS of DNTT on SiO_2 and CuO_x become larger with the increase of α as shown in Figure 2a and 2b. It indicated that DNTT on SiO_2 and CuO_x molecules have a standing configuration.

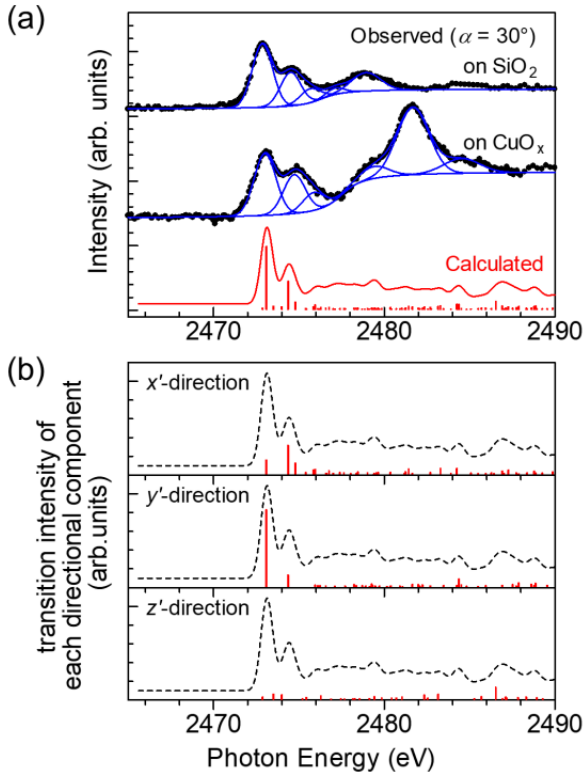

Figure 3. (a) Comparison between calculated and observed (α = 30°) S K-edge NEXAFS spectra of DNTT thin films. Observed spectra of 1.5-nm-thick DNTT films on SiO_2 and CuO_x were fitted with Gaussian peaks and a step-edge background. Raw (vertical bar diagram) and convoluted calculated data were shown in red color. The convolution curve is obtained with the Gaussian function (0.8eV-width). Calculated data rigidly shifted by 4.4 eV towards lower photon energy. (b) Transition intensity in each direction of the molecular coordinate. A dotted line in each panel, the same as the convolution curve in Figure 3a, is a guide for the eye.

Based on the above, a comparison between observed and theoretical incidence angle dependence of the transition intensity was shown in Figure 4. The observed intensities were provided by peak fitting with Gaussian peaks and a step-edge background. In the case of the 1.5-nm-thick thin film on SiO_2 as shown in Figure 4 (a), a combination of $\beta = 79°$ and $\Phi_M = 77°$ and 103°, suggesting a standing orientation, was obtained by the least-squares method. However, the obtained angle of β was slightly smaller than that of the (001) plane in the single crystal.[11] To explain the difference, flat-lying molecules and randomly oriented ones coexisting in the thin film were taken into account for the analysis of the polarization dependence. As the direction of the dipole transition is examined in NEXAFS, the averaged angle is obtained if the film contains the molecules with various orientations. The smaller β value could be explained by the small percentage of molecules with different orientations contained in the thin film. With the composition of 3% flat-lying molecules, theoretical values of 85° for β, and 77° and 103° for Φ_M showed good agreement with the observed polarization dependence of the film on SiO_2. Assuming random domains coexisting in the thin film, the composition of random domains was calculated to be 5%. From the fluctuation of ±5% in the observed intensities, we estimated the uncertainty in β and Φ_M as a range between minimal and maximal angles, resulting in 85° (84–87°) for β, and 77° (74–80°) and 103° (100–106°) for Φ_M. Thus, β and Φ_M of the standing molecule on SiO_2 were quantitatively determined within the experimental accuracy. It indicated that the 1.5-nm-thick thin film on SiO_2 was composed of a majority of molecules with standing orientation and a small amount of amorphous region.

Moreover, additional S K-edge NEXAFS spectra of a 6-nm-thick DNTT thin film on SiO_2, shown in Figure S4 (supporting information), were acquired in order to verify the result of the

1.5-nm-thick thin film on SiO_2. The first peak at 2473 eV and the second peak at 2475 eV were clearly detected in good agreement with the 1.5-nm-thick thin film. Similar to the discussion above, in the incidence angle dependence as shown in Figure 4b, the molecular orientation was determined to be a combination of 86° (84–90°) for β, and 73° (71–76°) and 107° (104–109°) for Φ_M under an assumption of the coexistence with the amorphous region consisting of 2% flat-lying molecules or 3% randomly oriented ones. Obtained angles were almost the same as the result of the 1.5-nm-thick thin film on SiO_2 within the experimental accuracy. We concluded that DNTT thin film on SiO_2 showed a well-ordered orientation at the growth of the monolayer.

The obtained β and Φ_M in this study were summarized with previous results reported by other groups in Table 1.[9,10,12] The result of the 1.5-nm-thick thin film on CuO_x was discussed later. In previous reports, the standing configuration of DNTT on SiO_2 was determined by means of C K-edge NEXAFS without any consideration of the rotation in the molecular plane.[9,10] Our results are consistent with the standing orientation of DNTT on SiO_2 and provide further information on Φ_M.

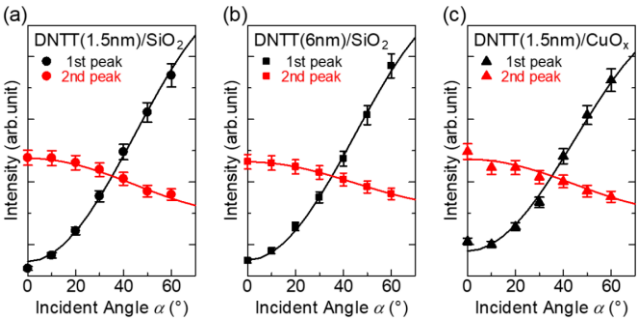

Figure 4. Comparison between observed and theoretical incidence angle (α) dependence of the transition intensity, (a) 1.5-nm-thick DNTT/SiO_2, (b) 6-nm-thick DNTT/SiO_2, and (c)

1.5-nm-thick DNTT/CuO_x. The observed data for 1.5-nm-thick DNTT/SiO_2, 6-nm-thick DNTT/SiO_2, and 1.5-nm-thick DNTT/CuO_x were plotted by closed circles, rectangles, and triangles, respectively. The theoretical data based on eqs 1, 2, and 3 were shown by solid lines.

Table 1. summary of β and Φ_M for DNTT thin films compared with previous works

Experimental technique	Sample	β [°]	Φ_M [°]	
S K-edge NEXAFS[c]	DNTT(1.5 nm)/SiO_2	85 (84–87)	77 (74–80), 103 (100–106)	This work
	DNTT(6 nm)/SiO_2	86 (84–90)	73 (71–76), 107 (104–109)	
	DNTT(1.5 nm)/CuO_x	84 (83–85)	73 (71–75), 107 (105–109)	
C K-edge NEXAFS	DNTT(30 nm)/SiO_2[a]	70–80	n/a	Ref. 9
	DNTT(0.3–5 nm)/SiO_2	85	n/a	Ref. 10
XRD	DNTT single crystal	85[b]	70, 110[b]	Ref. 12

[a] Deposited at 200–400 K.; [b] Values estimated from the CIF file in Supporting Information with assuming an arrangement of putting the (001) plane parallel to the substrate.; [c] Under an assumption of the coexistence with the minor component of amorphous region.

In a previous XRD analysis of DNTT single crystal,[12] the monoclinic unit cell of single crystal was composed of two nonequivalent molecules, forming a herringbone structure in the (001) plane and stacking layer by layer. DNTT molecules in the single crystal were arranged with β = 85° and Φ_M = 70° (110° for the other nonequivalent molecule) in the (001) plane. The molecular orientation in our result is consistent with this arrangement in the single crystal. From the resemblance in molecular orientation, the herringbone structure in the (001) plane parallel to the substrate can be similarly formed in the 1.5-nm-thick thin film on SiO_2. If a herringbone structure in the (001) plane of the film is formed, in-plane diffraction patterns can at least be detectable by XRD. Indeed, the XRD pattern of the 1.5-nm-thick thin film on SiO_2 revealed evidence for the herringbone structure as shown in Figure 5. Observed diffraction spots were marked by circles and indexed based on the reported single crystal structure.[12] No ring pattern originated from randomly oriented grains was observed. In parallel direction to the substrate, 110, 020, and 120 diffractions were observed. On the other hand, 100 and 010 diffractions marked by x-marks were not observed, which supports the herringbone arrangement (the projection of the structure along the molecular long axis belongs to the p2gg space group[29]). The lattice constants along the substrate plane were obtained as a = 0.62 nm and b = 0.78 nm, being in good agreement with that of the single crystal.[12] It indicated that DNTT molecules in the 1.5-nm-thick thin film formed the herringbone structure in (001) plane. Therefore, we concluded that the π-overlapped arrangement of the molecules could be optimized by the angles of both β and Φ_M. The crystalline-like molecular orientation formed in the 1.5-nm-thick thin film on SiO_2 could contribute to high carrier mobility in DNTT-based OFETs. Additionally, 001 diffraction detected along the substrate normal direction suggested a partially layered composition in the film,

revealing c = 1.61 nm and γ= 92.0±0.6°. The domain size was estimated to be 21.6 nm from the width of 001 diffraction spot.

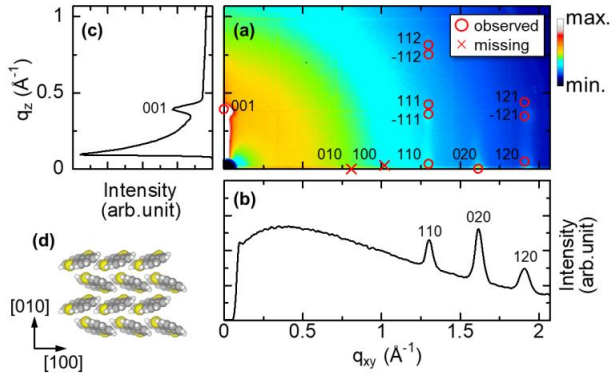

Figure 5. (a) Reciprocal space map from XRD measurement for a 1.5-nm-thick DNTT thin film on SiO_2. Observed diffraction spots were marked by red circles and indexed. 010 and 100 diffractions marked by x-marks were not observed. (b) and (c) show extracted line profiles along q_{xy}- and q_z-axis, respectively. (d) schematic image of the herringbone structure in (001) plane.

In the case of the 1.5-nm-thick DNTT thin film on CuO_x, the incidence angle dependence of the transition intensity was shown in Figure 4 (c). A combination of β = 74° and Φ_M = 73° and 107° was obtained for an averaged molecular orientation. The DNTT molecules on CuO_x revealed a smaller β angle and a similar Φ_M angle compared with those on SiO_2. Similar to the analysis of the film on SiO_2, the coexisting of flat-lying molecules in the thin film was assumed. As a result, 84° (83–85°) for β, and 73° (71–75°) and 107° (105–109°) for Φ_M were obtained for the 1.5-nm-thick thin film on CuO_x. The standing orientation was observed for the 1.5-nm-thick thin film on CuO_x similar to the film on SiO_2, suggesting a formation of the crystalline-like

molecular orientation. The composition of the flat-lying molecules on CuO_x was estimated to be 7%. Furthermore, the composition of random domains was calculated to be 12% of the thin film. These larger compositions on CuO_x than those on SiO_2 may be due to a larger surface roughness of the CuO_x substrate than that of the SiO_2 substrate. We concluded that the majority of DNTT molecules on CuO_x is in a standing orientation similar to the film on SiO_2. As discussed above, S K-edge NEXAFS has successfully provided the full information on the molecular orientation including Φ_M as well as β, which are important elements for the origin of the large transfer integral in DNTT thin film.

The application of our S K-edge NEXAFS approach is not limited to DNTT. As already discussed, the lack of LUMO population on the S atoms in DNTT[27] provided the large overlap of the wave functions between the S 1s inner shell and σ* molecular orbital involved in the C-S bond, revealing the anisotropic electron transition in the molecular plane. It enables us to evaluate the full information on the molecular orientation of DNTT. We can discuss the applicability of our approach based on the calculated LUMO population on the S atoms. For example, other thienothiophene-based molecules such as 2,7-dipheneyl[1]benzothieno[3,2-*b*]benzothiophene (DPh-BTBT) and dianthra[2,3-*b*:2',3'-*f*]thieno[3,2-*b*]thiophene (DATT) has a small LUMO population on the S atoms similar to DNTT.[13,30] The molecular orientations of these molecules can be fully determined only by S K-edge NEXAFS. On the other hand, the present method may not be applicable to [1]benzothineno[3,2-*b*]benzothiophene (BTBT)[30] and alkyl-substituted 2,7-dioctyl[1]benzothieno[3,2-*b*][1]benzothiophene (C_8-BTBT)[31] because of a significant population of the LUMO on the S atoms. The energy position of π* transition perpendicular to

the molecular plane may overlap with that of the σ* transition which makes it difficult to resolve the feature into the π* and σ* transitions. Indeed, the overlapped feature, which consists of π* and σ* transitions was observed in polycrystalline polythiophene[32] whose LUMO has a large population on the S atom.

Conclusion

In conclusion, we have demonstrated that S K-edge NEXAFS is suitable to analyze the full information of molecular orientation, the angles of tilting β and rotational Φ_M, in the DNTT thin films. Under the coexistence with a minor component of the amorphous region, molecular orientations of DNTT thin films on both SiO_2 and CuO_x substrates were evaluated using S K-edge NEXAFS. The angles of β and Φ_M in DNTT thin film on SiO_2 were similar to those in the (001) plane of the single crystal, revealing the herringbone structure. In the case of DNTT thin film on CuO_x, the majority of DNTT molecules were arranged in the standing orientation similar to that on SiO_2. Well-ordered orientations of DNTT are possible to enhance an optimized π-overlapped arrangement of the molecules in organic semiconductor devices. The present method is also applicable to S-containing molecules with a small LUMO population on the S atoms. Our results indicate feasibility to analyze the molecular orientation in detail in the actual device structure as thick as even one monolayer, contributing toward the optimization of the device fabrication.

Supporting Information

Theoretical derivation of the incident angle dependence in NEXAFS (PDF)

Simulation of NEXAFS intensities based on eqs 2 and 3 (PDF)

Ultraviolet photoelectron spectrum of 1.5-nm-thick DNTT/SiO_2 (PDF)

S K-edge NEXAFS Spectra of 6-nm-thick DNTT/SiO_2 (PDF)

Corresponding Author

*E-mail okudaira@faculty.chiba-u.jp (Koji K. Okudaira)

Author Contributions

K.I. and K.K.O. designed the study and experiments. Y.U. and K.H. performed NEXAFS experiments. K.I., Y.U., and K.K.O. analyzed and interpreted NEXAFS data. K.I. wrote the manuscript. H. Y. performed XRD experiments. K.I. analyzed and interpreted XRD data. H.Y., and K.K.O. revised the manuscript. All authors have given approval to the final version of the manuscript.

Notes

The authors declare no competing financial interest.

Acknowledgment

We are grateful to Dr. Iwao Shimoyama at Materials Sciences Research Center (MSRC), Japan Atomic Energy Agency for supporting NEXAFS measurement and stimulating comments. We are also thanks to Dr. Tomoyuki Koganezawa at Japan Synchrotron Radiation Research Institute (JASRI) and Prof. Itaru Osaka at Hiroshima University for supporting XRD experiment. NEXAFS and XRD were performed with the approvals of Photon Factory (Proposal No. 2017G173) and JASRI (Proposal No. 2017A1771), respectively. This work was financially supported by JSPS KAKENHI grant number 17K05050.

References

(1) Fukagawa, H.; Yamane, H.; Kataoka, T.; Kera, S.; Nakamura, M.; Kudo, K.; Ueno, N. Origin of the Highest Occupied Band Position in Pentacene Films from Ultraviolet Photoelectron Spectroscopy: Hole Stabilization versus Band Dispersion. *Phys. Rev. B* **2006**, *73*, 245310.

(2) Duhm, S.; Heimel, G.; Salzmann, I.; Glowatzki, H.; Johnson, R. L.; Vollmer, A.; Rabe, J. P.; Koch, N. Orientation-Dependent Ionization Energies and Interface Dipoles in Ordered Molecular Assemblies. *Nature Materials* **2008**, *7*, 326–332.

(3) Yamada, K.; Yanagisawa, S.; Koganezawa, T.; Mase, K.; Sato, N.; Yoshida, H. Impact of the Molecular Quadrupole Moment on Ionization Energy and Electron Affinity of Organic

Thin Films: Experimental Determination of Electrostatic Potential and Electronic Polarization Energies. *Phys. Rev. B* **2018**, *97*, 245206.

(4) Zhong, S.; Zhong, J. Q.; Wee, A. T. S.; Chen, W. Molecular Orientation and Electronic Structure at Organic Heterojunction Interfaces. *J. Electron Spectrosc. Relat. Phenom.* **2015**, *204*, 12–22.

(5) *The Molecule-Metal Interface*; Koch, N., Ueno, N., Wee, A. T. S., Eds.; Wiley-VCH: Weinheim, 2013; pp 119-151.

(6) Hasegawa, Y.; Yamada, Y.; Hosokai, T.; Koswattage, K. R.; Yano, M.; Wakayama, Y.; Sasaki, M. Overlapping of Frontier Orbitals in Well-Defined Dinaphtho[2,3-b:2',3'-f]Thieno[3,2-*b*]-Thiophene and Picene Monolayers. *J. Phys. Chem. C* **2016**, *120*, 21536–21542.

(7) Stöhr, J. *NEXAFS Spectroscopy*; Springer-Verlag: Berlin, 1992; pp.276–291.

(8) Breuer, T.; Klues, M.; Witte, G. Characterization of Orientational Order in π-Conjugated Molecular Thin Films by NEXAFS. *J. Electron Spectrosc. Relat. Phenom.* **2015**, *204*, 102–115.

(9) Jung, M.-C.; Leyden, M. R.; Nikiforov, G. O.; Lee, M. V.; Lee, H.-K.; Shin, T. J.; Takimiya, K.; Qi, Y. Flat-Lying Semiconductor–Insulator Interfacial Layer in DNTT Thin Films. *ACS Appl. Mater. Interfaces* **2015**, *7*, 1833–1840.

(10) Breuer, T.; Karthäuser, A.; Klemm, H.; Genuzio, F.; Peschel, G.; Fuhrich, A.; Schmidt, T.; Witte, G. Exceptional Dewetting of Organic Semiconductor Films: The Case of Dinaphthothienothiophene (DNTT) at Dielectric Interfaces. *ACS Appl. Mater. Interfaces* **2017**, *9*, 8384–8392.

(11) Takimiya, K.; Yamamoto, T.; Ebata, H.; Izawa, T. [1]Benzothieno[3,2-b][1]Benzothiophenes- and Dinaphtho[2,3-*b*:2′,3′-*f*]Thieno[3,2-*b*]Thiophene-Based Organic Semiconductors for Stable, High-Performance Organic Thin-Film Transistor Materials. *Thin Solid Films* **2014**, *554*, 13–18.

(12) Yamamoto, T.; Takimiya, K. Facile Synthesis of Highly π-Extended Heteroarenes, Dinaphtho[2,3-*b*:2’,3’-*f*]Chalcogenopheno[3,2-*b*]Chalcogenophenes, and Their Application to Field-Effect Transistors. *J. Am. Chem. Soc.* **2007**, *129*, 2224–2225.

(13) Takimiya, K.; Yamamoto, T.; Ebata, H.; Izawa, T. Design Strategy for Air-Stable Organic Semiconductors Applicable to High-Performance field-Effect Transistors. *Sci. Technol. Adv. Mater.* **2007**, *8*, 273–276.

(14) Kang, M. J.; Doi, I.; Mori, H.; Miyazaki, E.; Takimiya, K.; Ikeda, M.; Kuwabara, H. Alkylated Dinaphtho[2,3-*b*:2′,3′-*f*]Thieno[3,2-b]Thiophenes (C_n-DNTTs): Organic Semiconductors for High-Performance Thin-Film Transistors. *Adv. Mater.* **2011**, *23*, 1222–1225.

(15) Nakayama, K.; Hirose, Y.; Soeda, J.; Yoshizumi, M.; Uemura, T.; Uno, M.; Li, W.; Kang, M. J.; Yamagishi, M.; Okada, Y., et al. Patternable Solution-Crystallized Organic Transistors with High Charge Carrier Mobility. *Adv. Mater.* **2011**, *23*, 1626–1629.

(16) Uno, M.; Tominari, Y.; Yamagishi, M.; Doi, I.; Miyazaki, E.; Takimiya, K.; Takeya, J. Moderately Anisotropic Field-Effect Mobility in Dinaphtho[2,3-*b*:2′,3′-*f*]Thiopheno[3,2-*b*]Thiophenes Single-Crystal Transistors. *Appl. Phys. Lett.* **2009**, *94*, 223308.

(17) Haas, S.; Takahashi, Y.; Takimiya, K.; Hasegawa, T. High-Performance Dinaphtho-Thieno-Thiophene Single Crystal Field-Effect Transistors. *Appl. Phys. Lett.* **2009**, *95*, 022111.

(18) Yamamoto, T.; Takimiya, K. FET Characteristics of Dinaphthothienothiophene (DNTT) on Si/SiO_2 Substrates with Various Surface-Modifications. *Journal of Photopolymer Science and Technology* **2007**, *20*, 57–59.

(19) Yamagishi, M.; Soeda, J.; Uemura, T.; Okada, Y.; Takatsuki, Y.; Nishikawa, T.; Nakazawa, Y.; Doi, I.; Takimiya, K.; Takeya, J. Free-Electron-like Hall Effect in High-Mobility Organic Thin-Film Transistors. *Phys. Rev. B* **2010**, *81*, 161306(R).

(20) Xie, W.; Willa, K.; Wu, Y.; Häusermann, R.; Takimiya, K.; Batlogg, B.; Frisbie, C. D. Temperature-Independent Transport in High-Mobility Dinaphtho-Thieno-Thiophene (DNTT) Single Crystal Transistors. *Adv. Mater.* **2013**, *25*, 3478–3484.

(21) Zschieschang, U.; Ante, F.; Kälblein, D.; Yamamoto, T.; Takimiya, K.; Kuwabara, H.; Ikeda, M.; Sekitani, T.; Someya, T.; Blochwitz-Nimoth, J., et al. Dinaphtho[2,3-b:2′,3′-f]Thieno[3,2-b]Thiophene (DNTT) Thin-Film Transistors with Improved Performance and Stability. *Organic Electronics* **2011**, *12*, 1370–1375.

(22) Hofmockel, R.; Zschieschang, U.; Kraft, U.; Rödel, R.; Hansen, N. H.; Stolte, M.; Würthner, F.; Takimiya, K.; Kern, K.; Pflaum, J., et al. High-Mobility Organic Thin-Film Transistors Based on a Small-Molecule Semiconductor Deposited in Vacuum and by Solution Shearing. *Organic Electronics* **2013**, *14*, 3213–3221.

(23) Edelstein, D.; Heidenreich, J.; Goldblatt, R.; Cote, W.; Uzoh, C.; Lustig, N.; Roper, P.; McDevitt, T.; Motsiff, W.; Simon, A., et al. Full Copper Wiring in a Sub-0.25 μm CMOS ULSI Technology. International Electron Devices Meeting. IEDM Technical Digest, Washington, DC, USA, 1997, pp. 773-776.

(24) Takahashi, O.; Saito, K.; Mitani, M.; Yoshida, H.; Tahara, F.; Sunami, T.; Waki, K.; Senba, Y.; Hiraya, A.; Pettersson, L. G. M. Studies of the X-ray Absorption Spectra of Some Methylcyano Esters. *J. Electron Spectrosc. Relat. Phenom.* **2005**, *142*, 113–119.

(25) Hermann, K.; Pettersson, L. G. M.; Casida, M. E.; Daul, C.; Goursot, A.; Koester, A.; Proynov, E.; St-Amant, A.; Salahub, D. R.; Carravetta, V., et al. *StoBe-DeMon Version 3.3*; Stockholm-Berlin, 2014.

(26) Chawla, S. K.; Sankarraman, N.; Payer, J. H. Diagnostic Spectra for XPS Analysis of Cu–O–S–H Compounds. *J. Electron Spectrosc. Relat. Phenom.* **1992**, *61*, 1–18.

(27) Sánchez-Carrera, R. S.; Atahan, S.; Schrier, J.; Aspuru-Guzik, A. Theoretical Characterization of the Air-Stable, High-Mobility Dinaphtho[2,3-*b*:2’3’-*f*]Thieno[3,2-*b*]-Thiophene Organic Semiconductor. *J. Phys. Chem. C* **2010**, *114*, 2334–2340.

(28) Morikawa, E.; Saile, V.; Okudaira, K. K.; Azuma, Y.; Meguro, K.; Harada, Y.; Seki, K.; Hasegawa, S.; Ueno, N. Pendant Group Orientation of Poly(2-Vinylnaphthalene) Thin Film Surface Studied by Near-Edge X-ray Absorption Fine Structure Spectroscopy (NEXAFS) and Angle-Resolved Ultraviolet Photoelectron Spectroscopy (ARUPS). *J. Chem. Phys.* **2000**, *112*, 10476–10481.

(29) Yoshida, H.; Inaba, K.; Sato, N. X-ray Diffraction Reciprocal Space Mapping Study of the Thin Film Phase of Pentacene. *Appl. Phys. Lett.* **2007**, *90*, 181930.

(30) Niimi, K.; Shinamura, S.; Osaka, I.; Miyazaki, E.; Takimiya, K. Dianthra[2,3-*b*:2′,3′-*f*]Thieno[3,2-*b*]Thiophene (DATT): Synthesis, Characterization, and FET Characteristics of New π-Extended Heteroarene with Eight Fused Aromatic Rings. *J. Am. Chem. Soc.* **2011**, *133*, 8732–8739.

(31) Kobayashi, H.; Kobayashi, N.; Hosoi, S.; Koshitani, N.; Murakami, D.; Shirasawa, R.; Kudo, Y.; Hobara, D.; Tokita, Y.; Itabashi, M. Hopping and Band Mobilities of Pentacene, Rubrene, and 2,7-Dioctyl[1]Benzothieno[3,2-b][1]Benzothiophene (C_8-BTBT) from First Principle Calculations. *J Chem Phys* **2013**, *139*, 014707.

(32) Ikeura-Sekiguchi, H.; Sekiguchi, T. Unoccupied Electronic States in Polythiophene as Probed by XAS and RAS. *Surf. Interface Anal.* **2008**, *40*, 673–675.

TOC Graphic

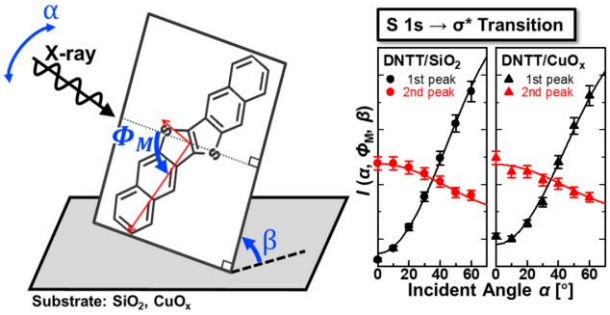
α
X-ray
Φ M
β
Substrate: SiO2, CuOx
S 1s → σ* Transition
DNTT/SiO2
1st peak
2nd peak
DNTT/CuOx
1st peak
2nd peak
I (α, Φ M, β)
0 20 40 60 0 20 40 60
Incident Angle α [°]